Talanta 212 (2020) 120764

Contents lists available at ScienceDirect

Talanta

journal homepage: www.elsevier.com/locate/talanta

Simultaneous detection of TNOS and P35S in transgenic soybean based on magnetic bicolor fluorescent probes

Yaqi Li[b], Nan Hao[a], Shilong Luo[c], Qian Liu[a], Li Sun[e], Jing Qian[a], Jianrong Cai[e,**], Kun Wang[a,d,*]

[a] Key Laboratory of Modern Agriculture Equipment and Technology, School of Chemistry and Chemical Engineering, Jiangsu University, Zhenjiang, 212013, China
[b] School of Grain Science and Technology, Jiangsu University of Science and Technology, Zhenjiang, 212003, China
[c] Sinograin Zhenjiang Grains & Oils Quality Testing Center, Zhenjiang, 212006, China
[d] Key Laboratory of Sensor Analysis of Tumor Marker, Ministry of Education, College of Chemistry and Molecular Engineering, Qingdao University of Science and Technology, Qingdao, 266042, China
[e] School of Food and Biological Engineering, Jiangsu University, Zhenjiang, 212013, China

ARTICLE INFO

Keywords:
Magnetic nanosphere
Fluorescent quantum dots
Genetically modified organism
Dual targets

ABSTRACT

A magnetic-separation-dual-targets fluorescent biosensor was fabricated to detect terminator nopaline synthase (TNOS) and promoter of cauliflower mosaic virus 35s (P35S) in transgenic soybean based on incorporation of bicolor CdTe quantum dots carried by silica nanospheres. In this protocol, the fixed probes for TNOS or P35S were magnetized firstly with Fe_3O_4@Au magnetic nanosphere by Au–S covalent bonding to achieve magnetized probes. Meanwhile, the capture probes for TNOS or P35S were functionalized with green or red fluorescent microspheres respectively to obtain fluorescently-labeled probes, which could emit relative strong green or red fluorescent signal. Two terminals of TNOS or P35S were recognized by magnetized probes and fluorescently-labeled probes respectively to form the sandwiched structures in the process of biosensor development subsequently, and it was separated by a magnet instantly. The fluorescence intensities of remnant supernatant were measured and analyzed accordingly to achieve simultaneous detection of TNOS and P35S. This biosensor exhibited a good dynamic range, low limit of detection and excellent selectivity in detecting transgenic soybean.

1. Introduction

With the increasing requirements of quantity and quality in crops, the genetically modified organisms (GMOs) has been a part of our daily food due to the desirable superiority such as delayed ripening, disease tolerance, virus resistance, insect resistance and providing better nutritional properties [1,2]. However, several controversies remain existent including the security of global ecology and the long-term influence of GMOs products on human beings. It was concluded that the GMOs and their foods have not obtained worldwide acceptance due to ethical concerns, public health safety and consumer mistrust resulting from environmental [3,4]. Basically, many countries have formulated a series of regulations and laws for GMOs labeling before being marketed and sold to make sure the right to be informed for consumers [5]. Consequently, both the enforcement of these labels and the predicament of actual supervision have requirements to develop detection methods for GMOs to address biosafety concerns.

The detection methods for GMOs mainly included protein-based and nucleic acid-based techniques [6,7]. The methods based on protein depend on the expression of target proteins, but the effortless denaturation by food processing for proteins is a fatal drawback [8,9]. As a result of the desirable superiority of high sensitivity, easy operability, excellent specificity, remarkable stability and good repeatability, these methods based on nucleic acid were attracted many attentions of researchers [6,10,11]. The mainly nucleic acid-based method for GMOs detection is polymerase chain reaction (PCR) combined with gel electrophoresis, but there are several acknowledged drawbacks, for instance, serious toxic, requisite laborious and time-consuming [12]. In order to overcome these issues, some biosensors were developed, such as electrochemical [13], quartz crystal microbalance (QCM) [14] and fluorescent [15] biosensor. However, lots of them were proposed to detect only one foreign DNA fragment in GMOs. As far as we know, there are three kinds of inserted exogenetic DNAs including the expression promoter, encoding region and expression terminator,

* Corresponding author. Key Laboratory of Modern Agriculture Equipment and Technology, School of Chemistry and Chemical Engineering, Jiangsu University, Zhenjiang, 212013, China.
** Corresponding author.
E-mail addresses: jrcai@ujs.edu.cn (J. Cai), wangkun@ujs.edu.cn (K. Wang).

https://doi.org/10.1016/j.talanta.2020.120764
Received 17 June 2019; Received in revised form 14 January 2020; Accepted 19 January 2020
Available online 20 January 2020
0039-9140/

respectively. Meanwhile, most of GMOs were approved and commercialized to utilize the promoter of the cauliflower mosaic virus 35s (P35S) and the terminator nopaline synthase (TNOS) gene sequence from *Agrobacterium tumefaciens*. Hence, it is significant to fabricate methods for multiple targets to improve the identification efficiency and achieve the fast detection for GMOs.

Magnetic nanospheres had been widely applied in the field of cell analysis [16], drug delivery [17], pathogens detection [18] and magnetic imaging [19] with the excellent superiority of easy magnetic separation, great specific surface area, fast reaction kinetics, rich functional sites and good biocompatibility. Meanwhile, the iron oxide nanoparticles (Fe_3O_4 NPs) as the classical magnetic nanomaterial had been demonstrated that it possessed the good properties of magnetic separation and strong carrying capacity [20,21]. Hence, the Fe_3O_4 NPs was employed to carry Au NPs to form the multifunctional core-shell composite nanoparticles of Fe_3O_4@Au magnetic nanospheres (MSPs) to exhibit both suitable intrinsic properties of Fe_3O_4 NPs and Au NPs [22]. And the MSPs had been applied to fabricate many kinds of methods to improve the detection sensitivity and reduce the time-cost which was attributing to their high quantity specific sites and excellent magnetic response ability [23,24].

Inspired by the above mentioned superiority of MSPs and excellent signal amplification of silica coated various CdTe quantum dots (QDs) to obtain the fluorescent nanopaticles (FNs) with different colors including green FNs (gFNs) and red FNs (rFNs) [25]. Meanwhile, biosensors exhibited excellent performances in quantitative detection [26,27]. In this work, a novel magnetic-separation-dual-targets biosensor was proposed for TNOS and P35S simultaneous detection for the first time. The MSPs were conjugated with thiol-modified corresponding fixed probes for TNOS (FT) or fixed probes for P35S (FP) through the strong affinity of Au–S to achieve MSPs-FT or MSPs-FP respectively. Meanwhile, the gFNs or rFNs were connected with amine-modified capture probes for TNOS (CT) or capture probes for P35S (CP) respectively by the amide reaction to obtain CT-gFNs or CP-rFNs which could be exhibited to strong relative fluorescent signal. These fixed probes and capture probes were recognized respectively by the corresponding targets DNA of TNOS or P35S due to the DNA specific hybridization to achieve the sandwich structure of MSPs-FT/TNOS/CT-gFNs and MSPs-FP/P35S/CP-rFNs to be separated by a magnet. Subsequently, the fluorescence intensities of the supernates were measured to realize the purpose of simultaneous detection for TNOS and P35S. The fabricated biosensor was employed to detect the genetically modified soybean samples which belonged to one of the most important GMOs, and the results of the detection were satisfactory, it was indicated that this proposed method was available and reliable.

2. Experimental section

2.1. Reagents and materials

(3-Aminopropyl) triethoxysilane (APTS), 1-Ethyl-3-(3-dimethylaminopropyl) carbodiimidehydro-chloride (EDC), N-hydroxysuccinimide (NHS), tris (2-chloroethyl) phosphate (TCEP) and 6-mercapto-1-hexanol (MCH) were purchased from Sigma-Aldrich. Tetraethylorthosilicate (TEOS), tris (hydroxymethyl)-aminomethane (Tris) were purchased from Sinopharm Chemical Reagent Co., Ltd. (Beijing, China). The transgenic soybean was provided by Sinograin Zhenjiang Grains & Oils Quaility Testing Center (Zhenjiang, China). The P35S and TNOS were used as the targets nucleotides sequences. EZ-10 spin column plant genomic DNA purification kit and all synthetic oligonucleotides were obtained from Sangon Biotech Co., Ltd. (Shanghai, China) (from 5′ to 3′) as shown in Table S1 (Supporting information).

2.2. Instrumentation

The transmission electron microscopy (TEM) images were taken by a JEOL 2100 TEM (JEOL, Japan) at 200 kV. UV–vis absorption spectra were recorded on a UV-2450 spectrophotometer (Shimadzu, Japan). The X-ray photoelectron spectroscopy (XPS) data were collected by an ESCALAB-MKII spectrometer with Mo Kα X-rays as the excitation source. FL spectra were measured on a Hitachi F-4500 fluorescence spectrophotometer (Tokyo, Japan). The agarose gel test was carried out by the sanheng DYY-12 gel-eletrophoresis (Beijing, China) and corresponding image was captured with image Labsoft version 5.1 (CA, USA).

2.3. Preparation the fixed probes-coupled MSPs to form MSPs-FT and MSPs-FP

The MSPs was prepared according to previous reports and shown in the supporting information and the fixed probes-coupled MSPs were synthesized as followed [28]. In brief, 1 mL FT (100 μM) was added into 1 mL Tris-HCl buffer (100 μM, pH 7.4) containing TCEP (200 mM). The mixed solution was stirred vigorously for 2 h at room temperature. After centrifuging the redundant TCEP, the fresh activated FT was added into 70 mL MSPs, and then the mixed solution was dispersed by sonication for 1 min and shocked gently for 1 h at 37 °C to obtain the MSPs-FT. MSPs-FT conjugations were separated by a magnet to remove the superabundant FT and washed by ultrapure water for 3 times, and ultrapure water with resistivity higher than 18.2 MΩ cm (Direct-Q UV, Millipore) was used throughout this work. 70 mL MCH (2 μM) was added into the obtained MSPs-FT and incubated for 1 h at 37 °C to block excess active sites. The final resultant MSPs-FT bioconjugates were acquire after magnetic separation and washing, and re-dispersed in 70 mL Tris-HCl buffer (100 μM, pH 7.4). The MSPs-FP bioconjugates were obtained through the similar operation with the concentration of FP (100 μM) rQDs. All the bioconjugates were saved at 4 °C for later use.

2.4. Preparation of capture probes-conjugated FNs

15 mL gFNs was added into 10 mL Tris-HCl buffer (100 μM, pH 7.4) containing EDC (20 mM) and NHS (10 mM) to stir for 2 h. 500 μL CT (100 μM) were introduced into the mixture and stirred for 12 h at the temperature of 37 °C. Subsequently, the gFNs-CT was obtained after centrifugation and washing for 3 times to remove the excess CT. It was re-dispersed in 15 mL Tris-HCl buffer (100 μM, pH 7.4). The rFNs-CP was acquired through the same operation with the rFNs and CP. Both of the gFNs-CT and rFNs-CP were stored at 4 °C for further use.

2.5. Determination of dual targets of TNOS and P35S

Both 0.5 mL gFNs-CT and 0.5 mL rFNs-CP were injected the mixture solution containing 1.5 mL MSPs-FT and 1.5 mL MSPs-FP. 100 μL various concentrations TNOS and P35S were introduced into the above solution. After incubation at 37 °C for 50 min, gFNs-CT/TNOS/MSPs-FT and rFNs-CP/P35S/MSPs-FP were separated instantly by a magnet placed. The supernatants were diluted to 5 mL to measure the fluorescent signal intensity.

2.6. The detection of TNOS and P35S in the real transgenic soybeans

The transgenic soybeans was grinded into a fine flour by the superpower food crusher. Subsequently, DNAs of samples were extracted from 100 mg preparation transgenic soybean flour using the Plant Genomic DNA Kit according to the manufacturer's instructions. The extracted DNA samples were amplified by the PCR method. The DNA samples of non-transgenic soybeans and the resultant PCR products which were diluted to 150, 100 and 50 times were used to be detected. Specifically, 100 μL of blank sample, non-transgenic soybeans DNA solution and three dilution concentrations of PCR products of transgenic soybeans extraction were respectively added into the above

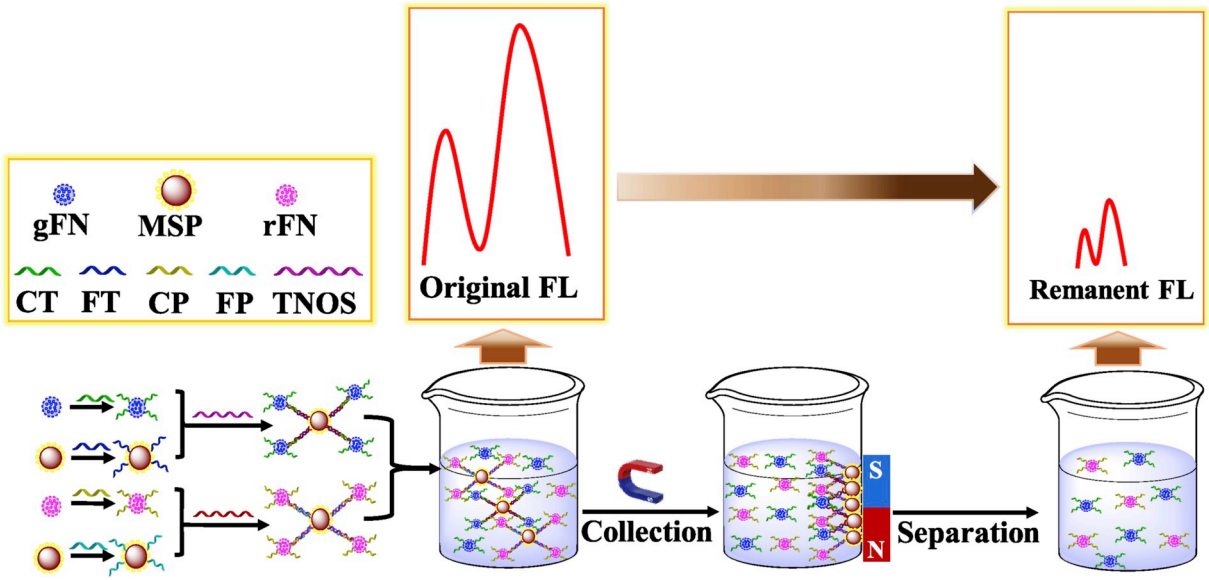

Fig. 1. Schematic illustration for magnetic-separation-dual-targets biosensor for TNOS and P35S simultaneous detection.

mentioned magnetic fluorescence biosensor, and measured the fluorescent intensities. Meanwhile, the corresponding results were verify by agarose gel electrophoresis and the obtained agarose gels was visualized with a UV light tray Gel Doc TM EZ System and the corresponding images was gained through Image Lab software version 5.0.

3. Results and discussion

3.1. Biosensor fabrication and detection principle

Owning to the excellent fluorescent property of QDs and the remarkable load capability of silica, the high-efficiency FNs were synthesized through employing the silica to carry abundant QDs to act the signal indicators. Meanwhile, the Fe_3O_4@Au MSPs with the strong magnetic properties were used to be the instrument to separate targets. Hence, the proposed strategy for TNOS and P35S simultaneous detection was illustrated in Fig. 1. The amine modified CT and CP were conjugated respectively on the gFNs and rFNs by the amido reaction to form the CT-gFNs and CP-rFNs. The sulfhydryl FT and FP were immobilized severally onto the surface of MSPs through Au–S covalent binding to constitute FT-MSPs and FP-MSPs. When the targets of TNOS and P35S were introduced, the two terminals of targets were respectively combined with the capture probes modified FNs and the fixed probes modified MSP to fabricate the sandwich structure nanocomposites through DNA specific hybridization. After a simple magnetic separation, the fluorescence intensities of the remnant supernatants were measured accordingly to detect the targets of TNOS and P35S simultaneously.

3.2. Characterization of the FNs

Fig. 2A and B were the TEM images of the as-prepared gQDs@SiO_2 and rQDs@SiO_2 respectively with the average diameter of 110 nm. As observed, these QDs@SiO_2 NPs were the roughly circular microspheres with a homogenized structure and smooth surface. After QDs were coated on the gQDs@SiO_2 and rQDs@SiO_2, some dark shadows were observed and the surfaces of gFNs (Fig. 2C) and rFNs (Fig. 2D) were rough obviously. In order to investigate the fluorescent property, the fluorescent intensity for gFNs and rFNs were compared to gQDs@SiO_2 and rQDs@SiO_2 respectively. It can be found the FL intensity of gFNs was 1.9 folds stronger than gQDs@SiO_2 (Fig. 2E) and the FL intensity of rFNs was 2.0 times stronger than rQDs@SiO_2 (Fig. 2F). Meanwhile, slight red shifts were observed in the peak emission of gFNs and rFNs respectively comparing with the gQDs@SiO_2 and rQDs@SiO_2, it might attribute to the strong combination between SiO_2 carried QDs and corresponding same color QDs. This demonstrated silicas carrying a large number of QDs in and on it [29]. This result confirmed that the as-prepared FNs had the excellent advantage of signal amplification.

3.3. Fabrication of the multifunctional biosensor

The characterization of $Fe_3O_4$and Fe_3O_4@Au MSPs were shown in supporting information. The DNA probes (curve a in Fig. 3A) exhibited an absorbance peak located at ~257 nm, which generated from the absorption of purine and thymine bases [30]. Compared with the DNA probes, both MSPs-FT (curve b in Fig. 3A) and MSPs-FP (curve c in Fig. 3A) had an additional peak at ~567 nm which corresponded to the UV absorption of Fe_3O_4@Au MSPs. It was shown as Fig. 3B and C, the gFNs (curve a in Fig. 3B) and rFNs (curve a in Fig. 3C) had the absorption peak at ~490 nm and ~597 nm respectively. After they conjugated the homologous DNA probes with CT and CP to form the CT-gFNs (curve b in Fig. 3C) and CP-rFNs (curve b in Fig. 3C), there were additional peaks at ~260 nm observed, which were accorded with the DNA absorption peak. Meanwhile, a little red shift was found, which might due to the strong binding interactions between the probes and FNs. To verify the successful assembly, the wide XPS spectra of CT-gFNs (curve a) and CP-rFNs (curve b) were measured as shown in Fig. 3D, which exhibited the elements of Si, Te, Cd, C, O, N, S, and P. The normalized XPS P 2p lines of CT-gFNs (curve a) and CP-rFNs (curve b) were shown in Fig. 3E. Compared with the gFNs (curve c) and rFNs (curve d), the CT-gFNs and CP-rFNs had the maximum signal at 133.2 eV, which was from the phosphate backbones of DNA probes [31], confirming that the CT-gFNs and CP-rFNs were successfully fabricated.

3.4. Optimization of detection conditions

In order to generate a highly sensitive magnetic-separation biosensor with a low detection limits for TNOS and P35S, it was significant to optimize the experimental parameters [32]. In the procedure of optimizing conditions, the change rate fluorescence intensity was expressed by $R= (F_O - F)/F_O$, where F_o was the original fluorescence intensity of reaction system, F was the fluorescence intensity of supernatant liquid for targets hybridization reaction and magnetic separation. As a result of the temperature-dependent for DNA special

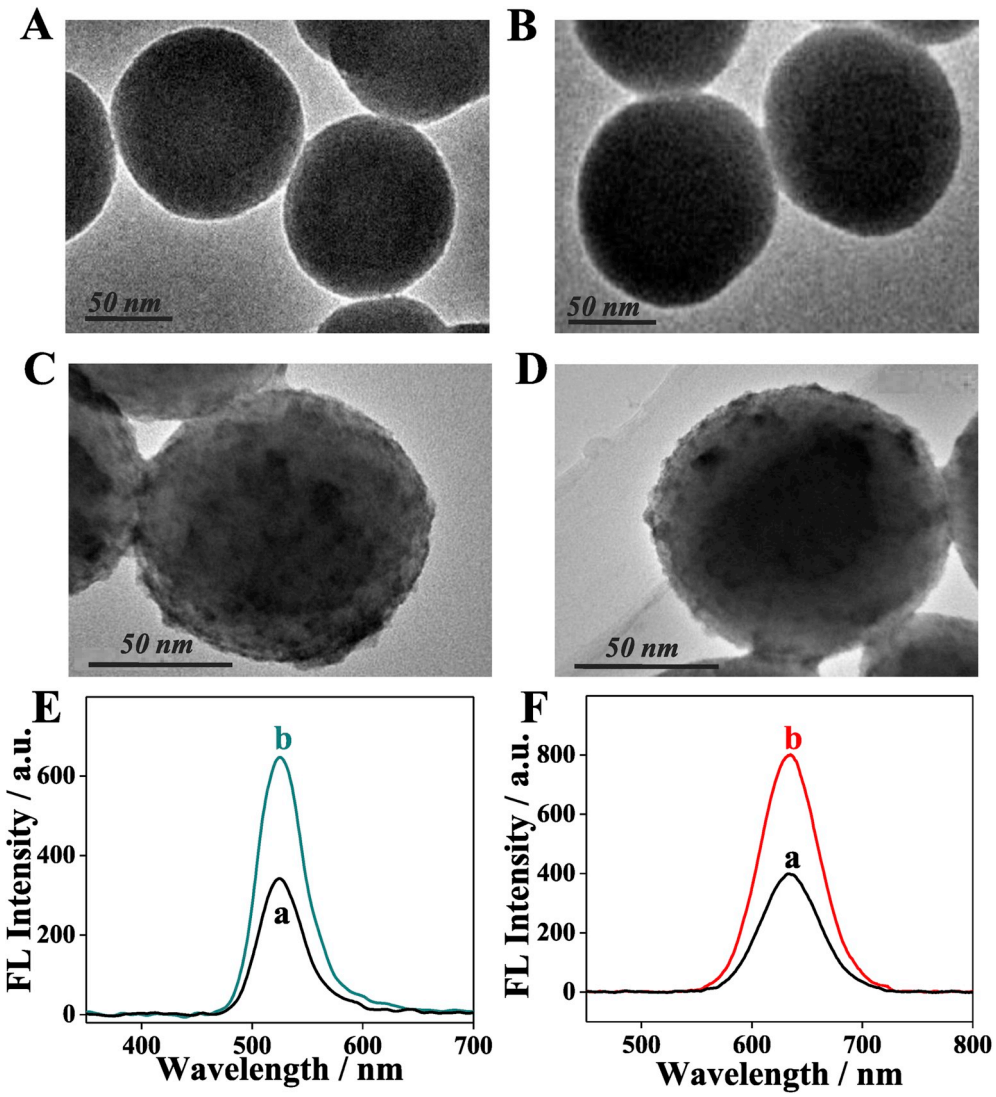

Fig. 2. TEM images of gQDs@SiO_2 (A), rQDs@SiO_2 (B), gFNs (C) and rFNs (D). Fluorescence spectra of (E) gQDs@SiO_2 (a) and gFNs (b), (F) rQDs@SiO_2 (a) and rFNs (b).

hybridization, it was necessary to optimize the solution temperature. As shown in Fig. S2A (Supporting information), the R value increased sharply with the solution temperature varied from 5 to 35 ˚C and there were obvious changes to been observed beyond 35 ˚C at the hybridization time of 50 min. Consequently, 35 ˚C was chosen as the incubation temperature. The pH value of solution was an important parameter for DNA hybridization and it was investigated from 6.0 to 8.5 which based on the physiological conditions. As can be seen in Fig. S2B, the R value increased with increasing pH value. And the R value became stable after the pH value of 7.4. Therefore, pH 7.4 was selected as the optimal solution pH value. In addition, the hybridization time between the target DNAs and probes had a direct bearing on the magnetic separation for targets. The hybridization time from 20 to 70 min were investigated according to the routine custom. As displayed in Fig. S2C, the R value increased gradually with the growing hybridization time and achieved a stable level at 50 min. This suggested that 50 min was enough and employed as the optimal hybridization time in the following detection.

3.5. Construction of magnetic-separation-dual-targets biosensor for TNOS and P35S detection

The sensing performance of this magnetic-separation-dual-targets biosensor was investigated by introducing a series of various concentrations of TNOS and P35S into the detection system under the optimized conditions. In this detection process, the fluorescence at 527 nm and 636 nm came from gFNs and rFNs respectively. The targets of TNOS and P35S were recognized by corresponding capture and fixed probes through the DNA special hybridization. Subsequently, the supernatants were separated by a magnet and measured the fluorescence intensities. As illustrated in Fig. 4A, with the concentrations of TNOS and P35S increasing, the fluorescence intensities decreased gradually, which was attributed to the targets of TNOS and P35S immobilized with gFNs and rFNs to be removed. This biosensor exhibited a good dynamic range of 0.2–800.0 nM for TNOS with the low limit of detection (LOD) of 0.07 nM and 0.1–800.0 nM for P35S with LOD of 0.04 nM (S/N = 3). Fig. 4B showed the linear regression analysis of TNOS detection with an R^2 value of 0.9816. Meanwhile, it was discovered that this biosensor displayed the reasonable linear relationship for P35S detection with an R^2 value of 0.9923 in Fig. 4C.

There are some electrochemical biosensor reported for transgenic soybean detection in recent years [33,34]. Compared with these electrochemical detection, our method needn't tedious procedure of electrode modification and exhibited good performance in simultaneous detection for TNOS and P35S. The relative materials and linear range was shown in Table 1 [35–41], this proposed magnetic-separation-dual-

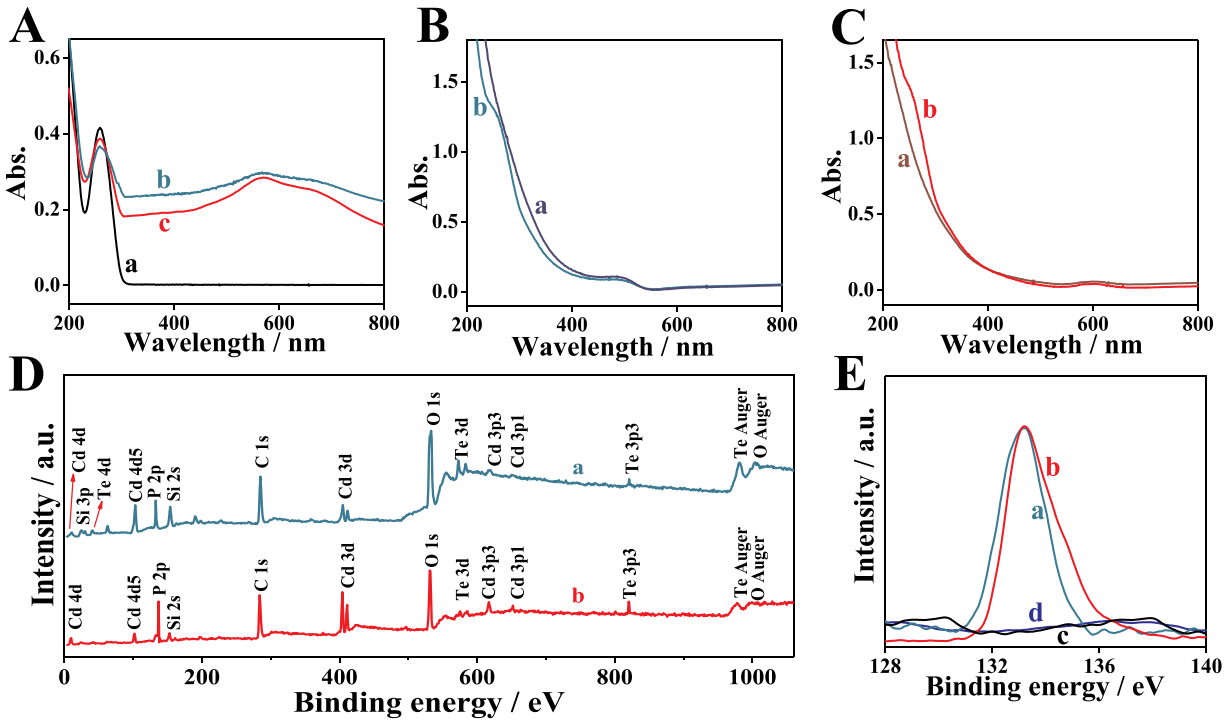

Fig. 3. (A) UV–vis spectra of DNA probes (a), MSPs-FT (b) and MSPs-FP (c). (B) UV–vis spectra of gFNs (a) and CT-gFNs (b). (C) UV–vis spectra of rFNs (a) and CP-rFNs (b). (D) XPS spectra of the CT-gFNs (a) and CP-rFNs (b). (E) XPS spectra of P 2p for CT-gFNs (a), CP-rFNs (b), gFNs (c) and rFNs (d).

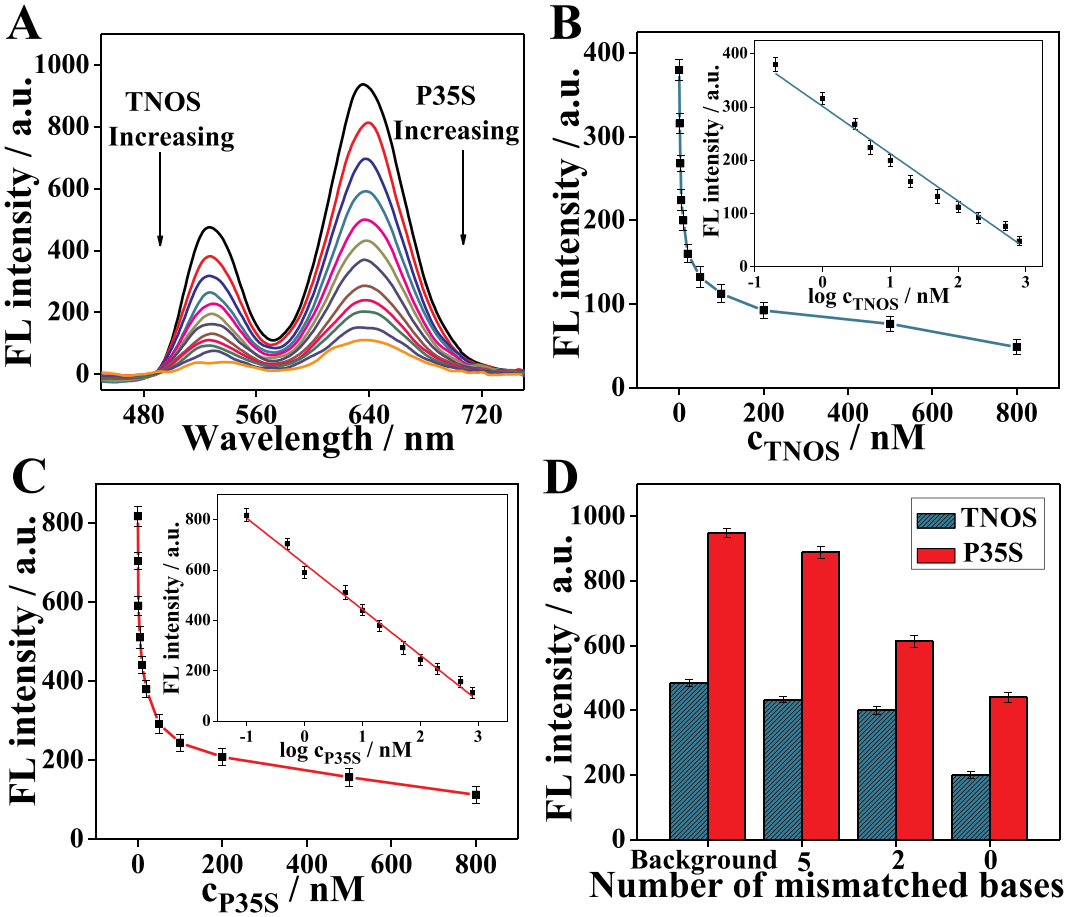

Fig. 4. (A) Fluorescence intensity for TNOS and P35S simultaneous detection. Linear regression analyses of detecting for TNOS (B) and P35S (C). (D) Fluorescence intensity with the decreased number of mutations on the targets.

Table 1
Comparison with the previous sensors for DNA detection.

Main materials	Linear range/LOD (nM)	References
GQDs[a]/CNs[b]	1.5–133.0/0.4	[35]
DNA-AgNCs[c]	5.0–350.0/1.3	[36]
AgNCs/MWCNTs[d]	31.0–2000.0/24.0	[37]
CdTe QDs[e]/CDs[f]	0–50.0/1.0	[38]
AgNCs/GO[g]	10.0–200.0/1.18	[39]
FAM/CNTs[h]	1.0–50.0/0.4	[40]
FAM/MPC[i]	3.0–150.0/1.0	[41]
QDs@SiO_2@QDs/Fe_3O_4@Au	0.2–800.0/0.07& 0.1–800.0/0.04	This work

[a] Graphene quantum dots.
[b] Carbon nanotubes.
[c] Silvernanoclusters.
[d] Multiwalled carbon nanotubes.
[e] Quantum dots.
[f] Carbon dots.
[g] Grapheneoxide.
[h] Carbon nanotubes.
[i] Magnetic porous carbon.

targets biosensor which was constituted by the SiO_2 carried in and on QDs and Fe_3O_4@Au MSPs exhibited a wider linear ranges and lower LODs. Meanwhile, it could be used for double targets simultaneous detection, which revealed the high efficiency than those single target detection methods. Therefore, all mentioned above indicated that this biosensor was more feasible and reliable for multiplex components detection in genetically modified organism.

3.6. Selectivity, accuracy, reproducibility and stability of this proposed biosensor

In order to investigate the selectivity of this proposed magnetic-separation-dual-targets biosensor, the fluorescence intensity of this biosensor for targets DNAs and corresponding mismatched bases DNA were evaluated. It was shown from Fig. 4D, the background was the original fluorescence intensity. With the decreasing of the number of the mismatched bases, the fluorescence intensity decreased gradually, which was attributed that the reduced mismatched bases could increase the amount of specific hybridize between targets and probes to separate the more gFNs and rFNs. This result demonstrated the excellent selectivity of this proposed biosensor toward dual targets of TNOS and P35S. The accuracy of the proposed biosensor was researched at concentrations of 50, 100, 200 nM of TNOS and P35S by detecting intra-assay variation and inter-assay variation. The results are shown in Table S2 (Supplementary Material). The biosensor gave acceptable intra-assay variation and inter-assay variation which were both < 10%, thereby demonstrating the high accuracy. In additionally, the reproducibility of this biosensor was investigated in five independent and repetitive experiments, the relative standard deviation (RSD) was found to be 6.2%, it illustrated the proposed approach possessed the good reproducibility. Meanwhile, the long-term stability of this biosensor was evaluated after 20 days storage at 4 °C. Compared with the initial value, the fluorescence intensity for 200 nM tDNAs was nearly 95.2% which can be attributed to the excellent load capacity of silicon, remarkable magnetic stability of MSPs and strong interaction of DNA specific hybridization. The result showed that this biosensor had the good long-term stability. These above-mentioned properties illustrated this proposed biosensor can be used for simultaneous detection of dual exogenous tDNAs.

3.7. Analytical application in real transgenic soybean samples

To estimate the practicability of this fabricated biosensor, the transgenic and non-transgenic soybean samples were used to be detected [42]. The DNA samples were extracted according to the instruction of DNA purification kit. This obtained DNA samples were amplified by PCR and confirmed by 2% agarose gel electrophoresis as shown in Fig. 5A. It was discovered that both TNOS and P35S were contained in this transgenic soybean sample. The resultant PCR products were diluted to 150, 100 and 50 times and detected by this proposed magnetic-separation-dual-targets biosensor respectively. It was seen in Fig. 5B, with the decreasing of dilution ratio, the fluorescence intensities reduced gradually, which was attributed to the increasing of targets concentration and the separation of the more FNs. Meanwhile, the data of analysis of TNOS and P35S in real transgenic soybean PCR product was shown in Table S3 (Supplementary material). The results were obtained from the equation of linear regression which was carried out though taking the experiment data of FL intensity into the corresponding regression equation. As can been seen from the results, when the diluted times of transgenic soybean PCR product was 50 times, the calculated concentration of transgenic fragment of TNOS and P35S was 343.98 nM and 343.22 nM respectively. With the increasing of diluted time, the calculated concentration of transgenic fragment decreased. When the diluted times added up to 150 times, the concentration of TNOS and P35S severally reduced to 0.61 nM and 0.39 nM, which demonstrated this proposed method could be applied to achieve the quantitative value of transgenic soybean. Therefore, this result indicated that this sensor can be used for dual targets of TNOS and P35S detection in real transgenic soybeans.

4. Conclusions

A novel and efficient magnetic-separation-dual-targets fluorescence biosensor had been established, which exhibited the remarkable performance of dual targets of TNOS and P35S detection simultaneously in transgenic soybean. By the benefits from DNA highly efficient hybridization, the two terminals of TNOS or P35S targets DNA can be

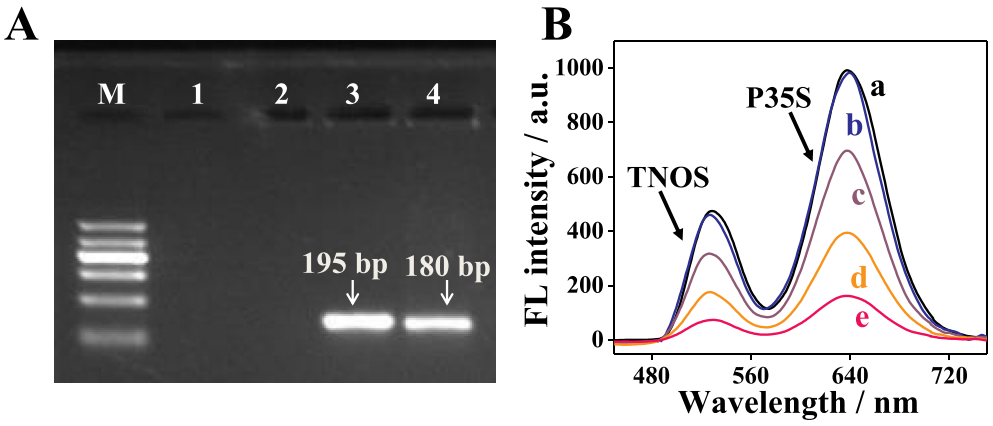

Fig. 5. (A) Confirmation of the TNOS and P35S in transgenic soybean by 2% agarose gel electrophoresis, (M) DNA markers, (1) blank control, (2) non-transgenic soybean, (3) P35S PCR product, (4) TNOS PCR product. (B) Results obtained from the testing of transgenic soybean samples, (a) blank, (b) non-transgenic soybean, (c) 150 times diluted transgenic soybean PCR product, (d) 100 times diluted transgenic soybean PCR product, (e) 50 times diluted transgenic soybean PCR product.

recognized respectively by the corresponding magnetized fixed probes of MSPs-FT or MSPs-FP and functionalized captured probes of CT-gFNs or CP-rFNs, which could be exhibited the relative strong fluorescence to fabricate the sandwich structure of MSPs-FT/TNOS/CT-gFNs or MSPs-FP/P35S/CP-rFNs to be separated by a magnet to generate the variety of fluorescence intensity. This presented magnetic-separation-dual-targets biosensor had offered desirable properties, such as great selectivity, wide linear range, low LOD level of 0.07 nM for TNOS and 0.04 nM for P35S, simple construction and low cost. Meanwhile, the process of total assay took no more than an hour to achieve the detection of TNOS and P35S. All these mentioned above confirmed that this proposed method has the potential to become a feasible method for multiple DNA or the other hazardous substance detection in food quality control.

Acknowledgement

This work was financially supported by the National Natural Science Foundation of China (No. 21675066, 31901799). Research Foundation of Jiangsu University (No. 19KJB550006). Research Foundation of Zhenjiang Science and Technology Bureau (No. FZ2017068, NY2017012, GZ2017006). Research start-up fund offinancially supported Jiangsu Province (No. BE2016355). Foundation of Key Laboratory of Sensor Analysis of Tumor Marker, Ministry of Education, Qingdao University of Science and Technology (No. SATM201807).

Appendix A. Supplementary data

Supplementary data to this article can be found online at https://doi.org/10.1016/j.talanta.2020.120764.

References

[1] S. Meric, O. Cakir, N. Turgut-Kara, S. Ari, Detection of genetically modified maize and soybean in feed samples, Genet. Mol. Res. 13 (1) (2014) 1160–1168.
[2] Y. Li, L. Sun, J. Qian, L. Long, H. Li, Q. Liu, J. Cai, K. Wang, Fluorescent “on-off-on” switching sensor based on CdTe quantum dots coupled with multiwalled carbon nanotubes@ graphene oxide nanoribbons for simultaneous monitoring of dual foreign DNAs in transgenic soybean, Biosens. Bioelectron. 92 (2017) 26–32.
[3] X. Huang, C. Zhai, Q. You, H. Chen, Potential of cross-priming amplification and DNA-based lateral-flow strip biosensor for rapid on-site GMO screening, Anal. Bioanal. Chem. 406 (2014) 4243–4249.
[4] A. Bawa, K. Anilakumar, Genetically modified foods: safety, risks and public concerns-a review, J. Food Sci. Technol. 50 (2013) 1035–1046.
[5] N. Cheng, Y. Shang, Y. Xu, L. Zhang, Y. Luo, K. Huang, W. Xu, On-site detection of stacked genetically modified soybean based on event-specific TM-LAMP and a DNAzyme-lateral flow biosensor, Biosens. Bioelectron. 91 (2017) 408–416.
[6] Z. Yun, L. Peng, S. Huo, X. Wu, J. Zhou, H. Zhang, W. Li, C. Qi, G. Huang, Automicrofluidic thin-film chip for genetically modified maize detection, Food Control 80 (2017) 360–365.
[7] Y. Li, L. Sun, J. Qian, C. Wang, Q. Liu, E. Han, N. Hao, L. Zhang, J. Cai, K. Wang, A homogeneous assay for highly sensitive detection of CaMV35S promoter in transgenic soybean by förster resonance energy transfer between nitrogen-doped graphene quantum dots and Ag nanoparticles, Anal. Chim. Acta 948 (2016) 90–97.
[8] M. Fraiture, P. Herman, I. Taverniers, M. De Loose, D. Deforce, N. Roosens, Current and new approaches in GMO detection: challenges and solutions, BioMed Res. Int. 2015 (2015) 1–22.
[9] M. Mazzara, C. Paoletti, P. Corbisier, E. Grazioli, S. Larcher, G. Berben, M. De Loose, I. Folch, C. Henry, N. Hess, Kernel lot distribution assessment (KeLDA): a comparative study of protein and DNA-based detection methods for GMO testing, Food Anal. Methods 6 (2013) 210–220.
[10] S. Choi, Hexaplex PCR assay and liquid bead array for detection of stacked genetically modified cotton event 281-24-236 × 3006-210-23, Anal. Bioanal. Chem. 401 (2011) 647–655.
[11] J. Guo, L. Yang, L. Chen, D. Morisset, X. Li, L. Pan, D. Zhang, MPIC: a high-throughput analytical method for multiple DNA targets, Anal. Chem. 83 (2011) 1579–1586.
[12] D. Zhu, J. Liu, Y. Tang, D. Xing, A reusable DNA biosensor for the detection of genetically modified organism using magnetic bead-based electrochemiluminescence, Sens. Actuators, B 149 (2010) 221–225.
[13] N. Zhou, T. Yang, C. Jiang, M. Du, K. Jiao, Highly sensitive electrochemical impedance spectroscopic detection of DNA hybridization based on Au nano–CNT/PAN nano films, Talanta 77 (2009) 1021–1026.
[14] İ. Karamollaoğlu, H. Öktem, M. Mutlu, QCM-based DNA biosensor for detection of genetically modified organisms (GMOs), Biochem. Eng. J. 44 (2009) 142–150.
[15] B. Qiu, Y. Lin, Y. Lu, Z. Lin, K. Wong, G. Chen, A novel fluorescent biosensor for detection of target DNA fragment from the transgene cauliflower mosaic virus 35S promoter, Biosens. Bioelectron. 41 (2013) 168–171.
[16] B. Otieno, C. Krause, A. Latus, B. Chikkaveeraiah, R. Faria, J. Rusling, On-line protein capture on magnetic beads for ultrasensitive microfluidic immunoassays of cancer biomarkers, Biosens. Bioelectron. 53 (2014) 268–274.
[17] T. Anirudhan, D. Dilu, S. Sandeep, Synthesis and characterisation of chitosan crosslinked-β-cyclodextrin grafted silylated magnetic nanoparticles for controlled release of indomethacin, J. Magn. Magn. Mater. 343 (2013) 149–156.
[18] K. Chan, W. Ye, Y. Zhang, L. Xiao, P. Leung, Y. Li, M. Yang, Ultrasensitive detection of E. coli O157: H7 with biofunctional magnetic bead concentration via nanoporous membrane based electrochemical immunosensor, Biosens. Bioelectron. 41 (2013) 532–537.
[19] X. Yu, H. Xia, Z. Sun, Y. Lin, K. Wang, J. Yu, H. Tang, D. Pang, Z. Zhang, On-chip dual detection of cancer biomarkers directly in serum based on self-assembled magnetic bead patterns and quantum dots, Biosens. Bioelectron. 41 (2013) 129–136.
[20] H. Wang, Y. Li, A. Wang, M. Slavik, Sensitive and simultaneous detection of three food borne pathogens using magnetic nanobead–based immunoseparation and quantum dot–based multiplex immunoassay, J. Food Prot. 74 (2011) 2039–2047.
[21] Q. Wu, Y. Sun, D. Zhang, S. Li, X. Wang, D. Song, Magnetic field-assisted SPR biosensor based on carboxyl-functionalized graphene oxide sensing film and Fe_3O_4-hollow gold nanohybrids probe, Biosens. Bioelectron. 86 (2016) 95–101.
[22] H. Zhou, N. Gan, T. Li, Y. Cao, S. Zeng, L. Zheng, Z. Guo, The sandwich-type electrochemiluminescence immunosensor for α-fetoprotein based on enrichment by Fe_3O_4-Au magnetic nano probes and signal amplification by CdS-Au composite nanoparticles labeled anti-AFP, Anal. Chim. Acta 746 (2012) 107–113.
[23] Z. Wu, C. Zhou, J. Chen, C. Xiong, Z. Chen, D. Pang, Z. Zhang, Bifunctional magnetic nanobeads for sensitive detection of avian influenza A (H7N9) virus based on immunomagnetic separation and enzyme-induced metallization, Biosens. Bioelectron. 68 (2015) 586–592.
[24] J. Salado, M. Insausti, L. Lezama, I. De Muro, M. Moros, B. Pelaz, V. Grazu, J. De La Fuente, T. Rojo, Bifunctional magnetic nanobeads for sensitive detection of avian influenza A (H7N9) virus based on immunomagnetic separation and enzyme-induced metallization, Nanotechnology 23 (2012) 315102–315110.
[25] Y. Li, L. Sun, Q. Liu, E. Han, N. Hao, L. Zhang, S. Wang, J. Cai, K. Wang, Photoelectrochemical CaMV35S biosensor for discriminating transgenic from non-transgenic soybean based on SiO_2@ CdTe quantum dots core-shell nanoparticles as signal indicators, Talanta 161 (2016) 211–218.
[26] M. Masud, J. Na, M. Younus, M. Hossain, Y. Bando, M. Shiddiky, Y. Yamauchi, Superparamagnetic nanoarchitectures for disease-specific biomarker detection, Chem. Soc. Rev. 48 (2019) 1517–5751.
[27] Y. Li, S. Luo, L. Sun, D. Kong, J. Sheng, K. Wang, C. Dong, A green, simple, and rapid detection for Amaranth in candy samples based on the fluorescence quenching of nitrogen-doped graphene quantum dots, Food Ana. Methods 12 (2019) 1658–1665.
[28] Z. Zhou, W. Wei, Y. Zhang, S. Liu, DNA-responsive disassembly of AuNP aggregates: influence of nonbase-paired regions and colorimetric DNA detection by exonuclease III aided amplification, J. Mater. Chem. B 1 (2013) 2851–2858.
[29] J. Wang, X. Peng, D. Li, X. Jiang, Z. Pan, A. Chen, L. Huang, J. Hu, Ratiometric ultrasensitive fluorometric detection of ascorbic acid using a dually emitting CdSe@SiO_2@CdTe quantum dot hybrid, Microchim. Acta 185 (2018) 42–50.
[30] C. Wang, J. Qian, K. Wang, K. Wang, Q. Liu, X. Dong, C. Wang, X. Huang, Magnetic-fluorescent-targeting multifunctional aptasensorfor highly sensitive and one-step rapid detection of ochratoxin A, Biosens. Bioelectron. 68 (2015) 783–790.
[31] J. Wang, G. Liu, M. Engelhard, Y. Lin, Sensitive immunoassay of a biomarker tumor necrosis factor-alpha based on poly (guanine)-functionalized silica nanoparticle label, Anal. Chem. 78 (2006) 6974–6979.
[32] X. Xu, L. He, Y. Long, S. Pan, H. Liu, J. Yang, X. Hu, S-doped carbon dots capped ZnCdTe quantum dots for ratiometric fluorescence sensing of guanine, Sens. Actuators, B 279 (2019) 44–52.
[33] D. Chen, M. Zhang, M. Ma, H. Hai, J. Li, Y. Shan, A novel electrochemical DNA biosensor for transgenic soybean detection based on triple signal amplification, Anal. Chim. Acta 1078 (2019) 24–31.
[34] A. Plácido, C. Pereirab, A. Guedesc, M. Barrosoa, R. Miranda-Castrod, N. Álvarezd, C. Delerue-Matos, Electrochemical genoassays on gold-coated magnetic nanoparticles to quantify genetically modified organisms (GMOs) in food and feed as GMO percentage, Biosens. Bioelectron. 110 (2018) 147–154.
[35] Z. Qian, X. Shan, L. Chai, J. Ma, J. Chen, H. Feng, DNA nanosensor based on biocompatible graphene quantum dots and carbon nanotubes, Biosens. Bioelectron. 60 (2014) 64–70.
[36] M. Hosseini, S. Mohammadi, Y. Borghei, M. Ganjali, Detection of p53 gene mutation (Single-Base mismatch) using a fluorescent silver nanoclusters, J. Fluoresc. 27 (2017) 1–6.
[37] W. Wang, L. Zhan, Y. Du, F. Leng, Y. Chang, M. Gao, C. Huang, Label-free DNA detection on the basis of fluorescence resonance energy transfer from oligonucleotide-templated silver nanoclusters to multi-walled carbon nanotubes, Anal. Method. 5 (2013) 5555–5559.
[38] S. Liang, L. Qi, R. Zhang, M. Jin, Z. Zhang, Ratiometric fluorescence biosensor based on CdTe quantum and carbon dots for double strand DNA detection, Sens. Actuators, B 244 (2017) 585–590.
[39] S. Zhang, K. Wang, K. Li, W. Shi, W. Jia, X. Chen, T. Sun, D. Han, A DNA-stabilized silver nanoclusters/graphene oxide-based platform for the sensitive detection of DNA through hybridization chain reaction, Biosens. Bioelectron. 91 (2017) 374–379.
[40] Q. Liao, B. Wei, L. Luo, Aptamer based fluorometric determination of kanamycin using double-stranded DNA and carbon nanotubes, Microchim. Acta 184 (2017) 627–632.
[41] H. Tan, G. Tang, Z. Wang, Q. Li, J. Gao, S. Wu, Magnetic porous carbon nanocomposites derived from metal-organic frameworks as a sensing platform for DNA fluorescent detection, Anal. Chim. Acta 940 (2016) 136–142.
[42] P. Manzanares, I. Mafra, J. Costa, M. Barroso, N. De-los-Santos-Álvarez, D. Cristina, M. Oliveira, M. Lobo-Castãnón, L. Beatriz, Electrochemical magnetoassay coupled to PCR as a quantitative approach to detect the soybean transgenic event GTS40-3-2 in foods, Sens. Actuators, B 222 (2016) 1050–1057.